Absorption changes in Photosystem II in the Soret band region upon the formation of the chlorophyll cation radical $[P_{D1}P_{D2}]^+$.

Alain Boussac[1], Miwa Sugiura[2], Makoto Nakamura[2], A. William Rutherford[3], Stefania Viola[3], Julien Sellés[4]

[1] Institut de Biologie Intégrative de la Cellule, UMR9198, CEA Saclay, 91191 Gif-Sur-Yvette, France

[2] Proteo-Science Research Center, and Department of Chemistry, Graduate School of Science and Technology, Ehime University, Bunkyo-cho, Matsuyama, Ehime 790-8577, Japan.

[3] Department of Life Sciences, Imperial College, SW7 2AZ London, UK

[4] Institut de Biologie Physico-Chimique, UMR CNRS 7141 and Sorbonne Université, 13 rue Pierre et Marie Curie, 75005 Paris, France.

e-mails :

alain.boussac@cea.fr , a.rutherford@imperial.ac.uk , s.viola@imperial.ac.uk , selles@ibpc.fr , miwa.sugiura@ehime-u.ac.jp, nnakamurammakoto@gmail.com

Abstract

Flash-induced absorption changes in the Soret region arising from the $[P_{D1}P_{D2}]^+$ state, the chlorophyll cation radical formed upon excitation of Photosystem II (PSII), were obtained using Mn-depleted PSII cores at pH 8.6. Under these conditions, Tyr_D is reduced before the first flash but oxidised before subsequent flashes. When $Tyr_D^\bullet$ is present, an additional signal in the $[P_{D1}P_{D2}]^+$-*minus*-$[P_{D1}P_{D2}]$ difference spectrum was observed when compared to the first flash. The additional feature was W-shaped with troughs at 434 nm and 446 nm. This feature was absent when Tyr_D was reduced, but was present when Tyr_D was physically absent (and replaced by phenylalanine) or when its H-bonding histidine (D2-His190) was physically absent (replaced by a Leucine),. Thus, the simple difference spectrum without the double trough feature at 434 nm and 446 nm, required the native structural environment around the reduced Tyr_D and its H

bonding partners to be present. A range of PSII variants were surveyed, and we found no evidence of involvement of P_{D1}, Chl_{D1}, Phe_{D1}, Phe_{D2}, Tyr_Z, and the Cytb_{559} heme in difference spectrum. Direct data ruling out the participation of P_{D2} is lacking. It seems possible that the specific H-bonding environment of around reduced Tyr_D allows a more homogenous electrostatic environment for $[P_{D1}P_{D2}]^+$. A role for P_{D2} in the double-trough Soret signal may be tested using mutants of P_{D2} axial His ligand D2-His197.

Introduction

Oxygenic photosynthesis is responsible for most of the energy input to life on Earth. This process converts the solar energy into fiber, food and fuel occurs in cyanobacteria, algae and plants. Photosystem II (PSII), the water-splitting enzyme, is at the heart of this process, see (Cox et al. 2020) for a recent review.

Mature cyanobacterial PSII generally consists of 20 subunits with 17 trans-membrane and 3 extrinsic membrane proteins. PSII binds 35 chlorophylls *a* (Chl-*a*), 2 pheophytins (Phe), 1 membrane b-type cytochrome, 1 extrinsic c-type cytochrome, 1 non-heme iron, 2 plastoquinones (Q_A and Q_B), the Mn_4CaO_5 cluster, 2 Cl^-, 12 carotenoids and 25 lipids (Suga et al. 2015). The 4th extrinsic PsbQ subunit was also found in PSII from *Synechocystis* sp. PCC 6803 in addition to PsbV, PsbO and PsbU (Gisriel et al. 2022).

Among the 35 Chls, 31 are antenna Chls and 4 (P_{D1}, P_{D2}, Chl_{D1} and Chl_{D2}), together with the 2 Phe molecules, constitute the reaction center pigments of PSII. After the absorption of a photon by the antenna, the excitation energy is transferred to the photochemical trap that consists of the four Chls; P_{D1}, P_{D2}, Chl_{D1}, Chl_{D2}. After a few picoseconds, a charge separation occurs resulting in the formation of the $Chl_{D1}^+Phe_{D1}^-$ and then of the $[P_{D1}P_{D2}]^+Phe_{D1}^-$ radical pair states, with the positive charge mainly located on P_{D1}, *e.g.* (Holzwarth et al. 2006, Romero et al. 2017). The main PSII cofactors are shown in Fig. 1.

After the formation of $[P_{D1}P_{D2}]^+Phe_{D1}^-$, the electron on Phe_{D1}^- is transferred to Q_A, the primary quinone electron acceptor, and then to Q_B, the second quinone electron acceptor. While Q_A is only singly reduced under normal conditions, Q_B accepts two electrons and two protons before leaving its binding site and being replaced by an oxidized plastoquinone molecule from the membrane plastoquinone pool (Boussac et al. 2010, de Causmaecker et al. 2019, Fufezan et al. 2005, Sedoud et al. 2011 and references therein). On the donor side of PSII, P_{D1}^+ oxidizes Tyr_Z, the Tyr161 of the D1 polypeptide. The $Tyr_Z^\bullet$ radical is then reduced by the Mn_4CaO_5 cluster, *e.g.* (Lubitz et al. 2019) for a review. After four charge separations, the Mn_4CaO_5 cluster

accumulates four oxidizing equivalents and thus cycles through five redox states denoted S_0 to S_4. Upon formation of the S_4-state, two molecules of water are oxidized, the S_0-state is regenerated and O_2 is released (Joliot et al. 1969, Kok et al. 1970).

In O_2 evolving PSII with an intact Mn_4CaO_5 cluster, the electron transfer from Tyr_Z to P_{D1}^+ takes place in time ranges from tens of ns to tens of µs, *e.g.* (Renger 2012). The kinetics in the ns range are sometimes discussed in term of a pure electron transfer, whereas in the µs range they involve large proton relaxations in the H-bond network, *e.g.* (Renger 2012). The fast electron transfer from Tyr_Z to P_{D1}^+ occurs with a $t_{1/2}$ close to 20 ns (Brettel et al. 1984, Gerken et al. 1987). The µs to tens of µs phases correspond to proton movements in which the phenolic proton of the $Tyr_Z^\bullet$ radical moves, in a first step, onto the H-bonded His190 of the D1 polypeptide.

In Mn-depleted PSII, the electron transfer from Tyr_Z to P_{D1}^+ is strongly pH dependent (Conjeaud and Mathis 1980) with a $t_{1/2}$ of ~ 190 ns at pH 8.5 and ~ 2-10 µs at pH 6.5 (Faller et al. 2001). At pH 8.5, Tyr_D, the Tyr160 of the D2 polypeptide that is symmetrically positioned with respect to Tyr_Z (Fig. 1), is slowly reduced in the dark (Boussac and Etienne 1982) and becomes able to donate an electron to P_{D1}^+ with a $t_{1/2}$ of ~ 190 ns, similar to Tyr_Z donation (Faller et al. 2001). Consequently, at room temperature and pH 8.5, the reduced Tyr_D can donate an electron to P_{D1}^+ in approximately half of the centers upon a saturating ns flash in Mn-depleted PSII, while in the remaining half P_{D1}^+ is reduced by Tyr_Z. Based on the rate and the distance between TyrD and PD1 and PD2, it is considered that TyrD oxidation occurs by donation to P_{D2}^+, which shares the cation with P_{D1} by a redox equilibrium, $[P_{D1}^+P_{D2}] \leftrightarrow [P_{D1}P_{D2}^+]$, (Rutherford et al. 2004).

The difference spectra $(P_{D1}P_{D2})^+$-*minus*-$(P_{D1}P_{D2})$ measured in the blue region of the Chl absorption, and corrected for the contribution of Q_A^--*minus*-Q_A formation, shows a large bleaching of the Soret band at ~ 432 nm in wild type PSII (Diner et al. 2001). Additionally, the difference spectrum exhibits a negative feature between 440 nm and 460 nm. The origin of this additional spectral feature that is observed in both inactive PSII (Diner et al. 2001) and O_2-evolving PSII, *e.g.* (Sugiura et al. 2004), has not been determined. In this spectral region, the redox changes of several species, such as the Chls, cytochromes and amino acid radicals may give rise to absorption changes upon a charge separation event. However, the difference spectra recorded at time as short as 20 ns after an actinic ns laser flash and exhibiting the negative spectral the feature between 440 nm and 460 nm cannot originate from states other than those

with $[P_{D1}P_{D2}]^+$ present. Alternatively, band shifts of either Chl's or cytochromes or amino acid radical(s) induced by the formation of P_{D1}^+ may also contribute.

In the present work, we have recorded the $[P_{D1}P_{D2}]^+Q_A^-$-*minus*-$[P_{D1}P_{D2}]Q_A$ difference spectra in PSII from different cyanobacteria species and mutants (see Fig.1) in order to clarify the nature of the spectral feature between 440 nm and 460 nm. All the measurements were done in Mn-depleted PSII after a long dark-adaptation in order to measure the $[P_{D1}P_{D2}]^+Q_A^-$-*minus*-$[P_{D1}P_{D2}]Q_A$ difference spectra with Tyr_D either reduced or oxidized, *i.e.* in the presence of $Tyr_D^\bullet$.

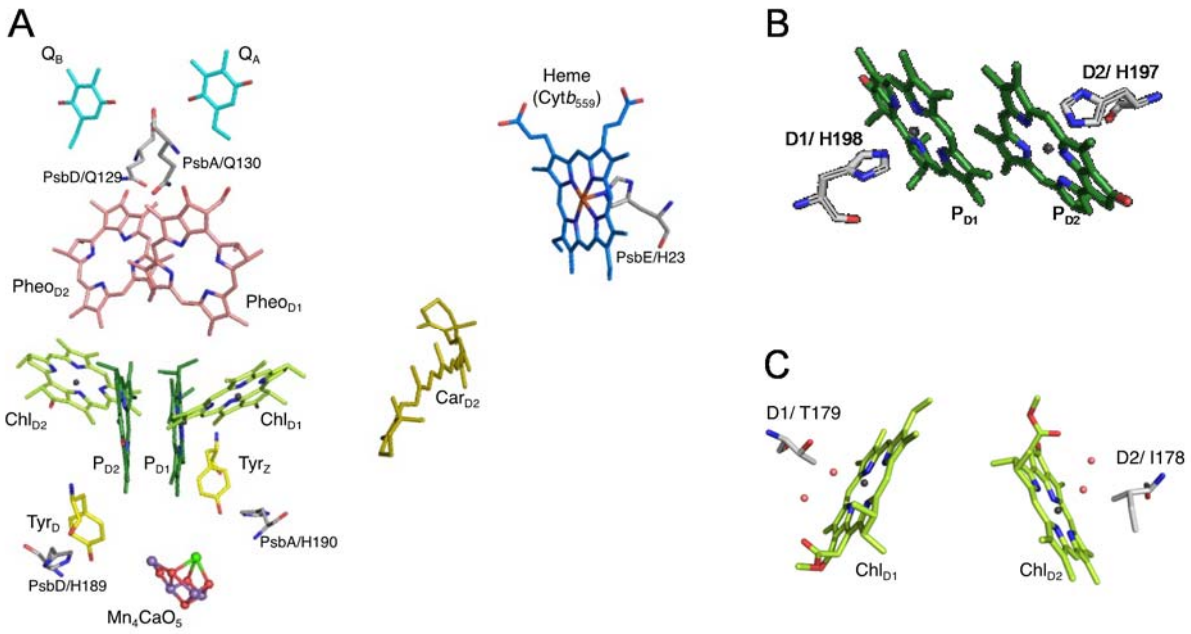

Figure 1: Panel A: Arrangement of cofactors of the T. elongatus PSII involved in the electron transfers and studied in the present work together with some amino acids interacting with these cofactors. D1/E130, corresponding to the situation occurring in the T. elongatus D1 isoform PsbA3, was drawn by substituting E130 for Q130 in the PDB 4UB6 structure in which D1 is the isoform PsbA1. Panel B, structure of P_{D1} and P_{D2} with their amino acid residue ligands. Panel C, structure around Chl_{D1} and Chl_{D2}. The figures were drawn with MacPyMOL with the A monomer in PDB 4UB6 (Suga et al. 2015).

Materials and Methods

PSII samples.

The PSII samples used in this study were purified from *i*) *Thermosynechoccocus elongatus* and *ii*) *Chroococcidiopsis thermalis* PCC7203 grown under far-red light (750 nm). PSII from *C. thermalis* has 4 Chl-*f* and 1 Chl-*d* replacing 5 of the 35 Chl-*a* (Nürnberg et al. 2018, Judd et al. 2020) see also (Chen et al. 2010, Gan et 2014, Gisriel et al. 2022b).

The *T. elongatus* strains used in this study, listed in Table 1, were constructed from a strain with a His_6-tag on the carboxy terminus of CP43, called 43H, in which the D1 protein is PsbA1.

Table 1: PSII samples used in this study

Parent strain [a]	nature of D1 [d]	mutation or modification	reference
43H	PsbA1	PsbA1	Sugiura and Inoue 1999
WT*1 [b]	PsbA1	PsbA1	Ogami et al. 2012
WT*3 [c]	PsbA3	PsbA3	Sugiura et al. 2008
WT*3 [c]	PsbA3	PsbA3/H198Q	Sugiura et al. 2016
WT*3 [c]	PsbA3	PsbA3/T179H	Takegawa et al. 2019
WT*3 [c]	PsbA3	PsbA3/E130Q	Sugiura et al. 2014
WT*3-Δ*psbD1* [c]	PsbA3	PsbD2/I178T	in preparation
WT*3 [c]	PsbA3	PsbE/H23A	Sugiura et al. 2015
43H-Δ*psbD1*	PsbA1	PsbD2/Y160F	Sugiura et al. 2004
43H-Δ*psbD1*	PsbA1	PsbD2/H189L	Un et al. 2007
43H-Δ*psbD1*	PsbA1	PsbD2/Y160F-H189L	unpublished
43H	PsbA1	+ 3-fluorotyrosine	Rappaport et al. 2009
FR *C. thermalis*	PsbA3	1 Chl-*d* and 4 Chl-*f*	Nürnberg et al. 2018

[a] T. elongatus strains in which the mutations/modifications have been done. The asterisk (*) indicates that the CP43 has a His_6 tag on the carboxy terminus. [b] ΔpsbA2-ΔpsbA3 strain. [c] ΔpsbA1-ΔpsbA2 strain. [d] The nature of the D1 protein has been controlled in purified PSII by recording the Qx band shift of Phe_{D1} upon Q_A^- formation, e.g. (Giorgi et al. 1996).

PSII purifications from the *T elongatus* strains were performed as previously described (Sugiura et al. 2014). For Mn-depletion, 20 mM NH_2OH, from a stock at 1 M at pH 6.5, and 1 mM EDTA were added to the PSII samples. Then, the hydroxylamine and EDTA were removed

by washings of the PSII samples by cycles of dilution in 1 M betaine, 15 mM $CaCl_2$, 15 mM $MgCl_2$, 40 mM MES, pH 6.5, followed by concentration using Amicon Ultra-15 centrifugal filter units (cut-off 100 kDa) until the estimated residual NH_2OH concentration was lower than 0.1 µM in the concentrated PSII samples before the final dilution for the ΔI/I measurements. In the final dilution step, the PSII samples were suspended in 1 M betaine, 15 mM $CaCl_2$, 15 mM $MgCl_2$, 100 mM Tris, pH 8.6.

The PSII from *C. thermalis* grown under far-red light was purified as previously described (Nürnberg et al. 2018) also treated with NH_2OH as described above.

UV-visible time-resolved absorption change spectroscopy.

Absorption change measurements were performed with a lab-built spectrophotometer (Béal et al. 1999) in which the absorption changes were sampled at discrete times after the actinic flash by short analytical flashes. These analytical flashes were provided by an optical parametric oscillator (Horizon OPO, Amplitude Technologies) pumped by a frequency tripled Nd:YAG laser (Surelite II, Amplitude Technologies), producing monochromatic flashes (355 nm, 2 nm full-width at half-maximum) with a duration of 5 ns. Actinic flashes were provided by a second Nd:YAG laser (Surelite II, Amplitude Technologies) at 532 nm, which pumped an optical parametric oscillator (Surelite OPO plus) producing monochromatic saturating flashes at 695 nm with the same pulse-length. The two lasers were working at a frequency of 10 Hz and the time delay between the laser delivering the actinic flashes and the laser delivering the detector flashes was controlled by a digital delay/pulse generator (DG645, jitter of 1 ps, Stanford Research). The path-length of the cuvette was 2.5 mm.

For the ΔI/I measurements, the Mn-depleted PSII samples were diluted in a medium with 1 M betaine, 15 mM $CaCl_2$, 15 mM $MgCl_2$, and 100 mM Tris with the pH adjusted with HCl at pH 8.6. The PSII samples from *T. elongatus* were dark-adapted for ~ 3-4 h at room temperature (20–22°C) before the addition of 0.1 mM phenyl *p*–benzoquinone (PPBQ) dissolved in dimethyl sulfoxide. The Mn-depleted PSII from *C. thermalis* were dark-adapted for ~2 h on ice before the addition of PPBQ. This is because we expected the PSII isolated from the mesophilic *C. thermalis* to be less stable at room temperature compared to the PSII isolated from the thermophilic *T. elongatus*. In all cases, the chlorophyll concentration of the samples was ~ 25 µg of Chl ml^{-1}. After the ΔI/I measurements, the absorption of each diluted batch of samples was precisely controlled to avoid errors due to the dilution of concentrated samples and the ΔI/I

values shown in the figures were normalized to A_{673} = 1.75, with ε ~ 70 $mM^{-1} \cdot cm^{-1}$ at 674 nm for dimeric *T. elongatus* PSII (Müh and Zouni 2005).

Results and Discussion

Fig. 2 shows the observation that triggered this study. In this experiment, the ΔI/I was measured from 401 to 457 nm, 20 ns after each of a series of 10 saturating ns laser flashes fired at 2 s time intervals, in a Mn-depleted PsbA3/PSII which was dark adapted for ~ 3-4 h at pH 8.6. This long dark-incubation allows Tyr_D to be reduced in the great majority of the centers (Boussac and Etienne 1982, Faller et al. 2001). The black spectrum was recorded after the first flash, *i.e.* it corresponds to the formation of the $[P_{D1}P_{D2}]^+Q_A^-$ state when Tyr_D is not yet oxidized. The red spectrum is an average of the ΔI/I measured from the 5th to 10th laser flash illumination, *i.e.* it corresponds to the formation of the $[P_{D1}P_{D2}]^+Q_A^-$ state in the presence of $Tyr_D^\bullet$ after it is formed on the first actinic flash.

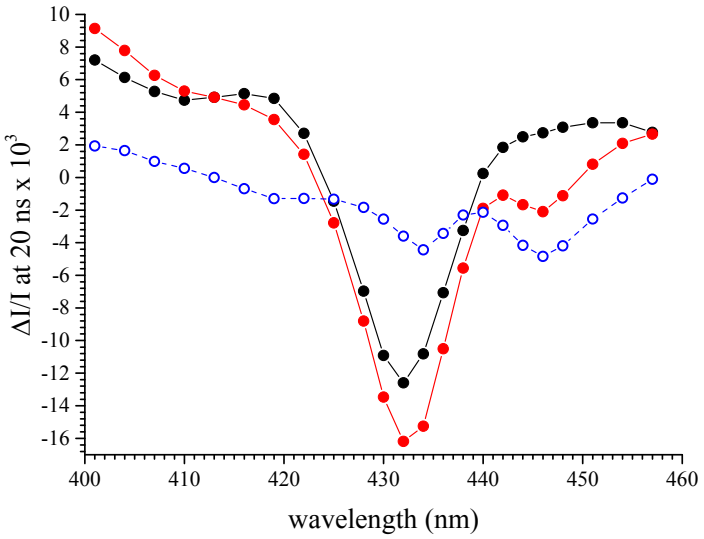

Figure 2: spectra recorded 20 ns after a laser flash illumination in Mn-depleted PsbA3-PSII which was dark-adapted for several hours at pH 8.6 to allow the reduction of Tyr_D. The black full circles were recorded after the 1st flash of a sequence of 10 flashes 2 s apart. The red full circles are the average the measurements done from the 5th to the 10th flash. The blue spectrum is the red spectrum minus the black spectrum. The Chl concentration was 25 µg/ml and 100 µM PPBQ was added before the measurements.

In Fig. 2, the maximum bleaching in the two spectra is at 432 nm as expected for the $[P_{D1}P_{D2}]^{+}$-*minus*-$[P_{D1}P_{D2}]$ difference spectrum (Diner et al. 2001). However, the two spectra differ significantly. The blue spectrum, which is the red spectrum *minus* the black spectrum, shows that, once $Tyr_D^{\bullet}$ has been formed after the first flashes, the $(P_{D1}P_{D2})^{+}Q_A^{-}$-*minus*-$(P_{D1}P_{D2})Q_A$ difference spectrum exhibits two additional negative features, with troughs at ~ 434 nm and ~ 446 nm (this difference spectrum was calculated assuming that the same amount of $(P_{D1}P_{D2})^{+}$ was formed in the two cases). The very small negative contribution at 446 nm in the black spectrum is most likely due to the small fraction of centers in which $Tyr_D^{\bullet}$ remained after the dark-adaptation. The trough at 434 nm in the blue spectrum could arise from the bleaching of the radical cation with a higher proportion of P_{D2}^{+}. However, this would imply a difference spectrum with a more derivative shape with a contribution of the band which disappears, something that is not observed. The difference has therefore a more complex origin.

Panel A in Fig. 3, shows the results of the same experiments as in Fig. 2 but using a Mn-depleted PsbA1-PSII. The results are very similar to those in Mn-depleted PsbA3-PSII, with the additional feature in the red spectrum presenting a trough at 446 nm. The major bleaching peaks at ~ 434 nm in the red spectrum, showing that the two troughs in the blue spectrum of Fig. 2 are also present here. The similarities of these results with those in Fig. 2 shows that the nature of PsbA, *i.e.* PsbA1 *vs* PsbA3, does not affect the formation and spectrum of the additional "W-shape" structure observed after the 5th to 10th flashes.

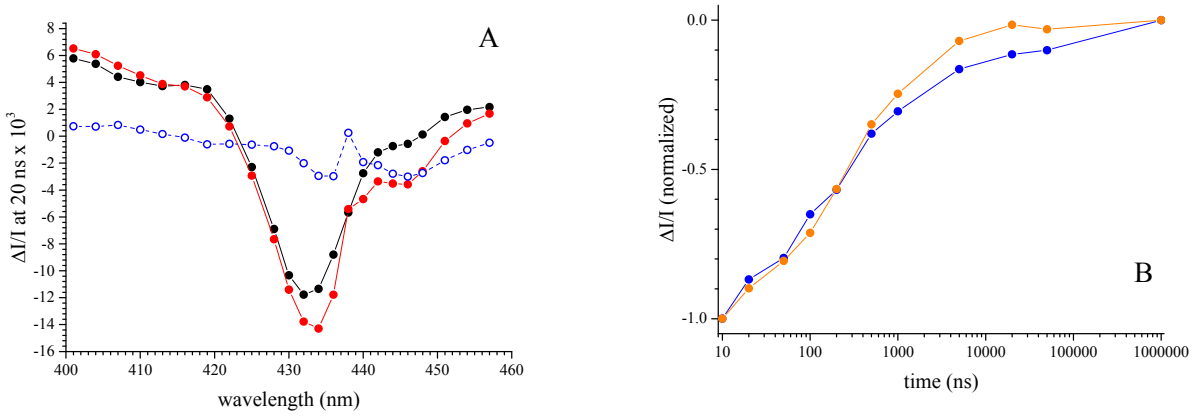

Figure 3: Panel A, spectra recorded 20 ns after a laser flash illumination in Mn-depleted PsbA1-PSII which was dark adapted for several hours at pH 8.6 to allow the reduction of Tyr_D. The black full circles were recorded after the 1st flash and the red full circles are the average the measurements done from the 5th to the 10th flash. The blue spectrum is the red spectrum minus the black spectrum. Panel B, decay kinetics measured from 10 ns to 1 ms in Mn-depleted PsbA1-PSII, either at 446 nm (orange) or at 432 nm (blue). The data points are averaged after

the 10th flash i.e. when all Tyr$_D^\bullet$ was formed in all centers. The amplitude of the decays between 10 ns and 1 ms was normalized to -1. The Chl concentration was 25 µg/ml and 100 µM PPBQ was added before the measurements.

Panel B in Fig. 3 shows the decay kinetics measured in the Mn-depleted PsbA1/PSII at 432 nm (blue points) and 446 nm (green points). This measurement was done after the 10th flash once Tyr$_D^\bullet$ was formed in all the centers. With the semi-logarithmic plot used in Panel B of Fig. 3, the decays at both 432 nm and 446 nm were almost linear from 10 ns to 1 µs and had a similar $t_{1/2}$ of ~ 200 ns. This $t_{1/2}$ value is very close to the value of 190 ns found previously (Faller et al. 2001, Rappaport et al. 2009).

The detection of the feature with troughs at 434 nm and 446 nm at times as short as 10-20 ns after the flash shows that it cannot originate from anything other than $[P_{D1}P_{D2}]^+$ or Q_A^- because the reduction of $[P_{D1}P_{D2}]^+$ and the oxidation of Q_A^- are not significant at that time ($t_{1/2}$ for $[P_{D1}P_{D2}]^+$ reduction ~200 ns, and for Q_A^- oxidation ~400 µs to 1 ms). As mentioned in the introduction, the "W-shape" structure between 440 nm and 460 nm was also observed in spectra after the removal of the Q_A^--*minus*-Q_A contribution (Diner et al. 2001). In addition, the decay with a $t_{1/2}$ of ~ 200 ns is much too fast to correspond to the forward electron transfer from Q_A^- to Q_B or Q_B^-, nor to charge recombination between Q_A^- and $[P_{D1}P_{D2}]^+$ (~1ms). Furthermore, the $t_{1/2}$ of ~ 200 ns corresponds well with the kinetics for the electron transfer from Tyr$_Z$ or Tyr$_D$ to $[P_{D1}P_{D2}]^+$ (Faller et al. 2001]. Finally, this negative spectral feature is not observed after the first flash, while Q_A^- is also formed on this first flash, confirming that the spectral feature does not arise from Q_A^- itself.

These considerations argue strongly in favor of $[P_{D1}P_{D2}]^+$ rather than Q_A^- being the species responsible for the spectral feature between 440 nm and 460 nm. The question is now whether these absorption changes originate from the $[P_{D1}P_{D2}]^+$ species or if they originate from an electrochromic response of a pigment and/or cofactor induced by the formation of $[P_{D1}P_{D2}]^+$. In order to obtain information on this subject we have recorded the $[P_{D1}P_{D2}]^+$-*minus*-$[P_{D1}P_{D2}]$ difference spectra in various types of PSII with mutations known to affect some of the cofactors in the vicinity of P_{D1}.

The first of these PSII was the Tyr$_D$-less mutant (Sugiura et al. 2004). The experiment in Figure 2 shows the W-shaped double trough feature at 434 nm and 446 nm is absent when Tyr$_D$ is reduced and present when Tyr$_D^\bullet$ is present. It therefore seemed possible that this feature arises from an absorption change in Tyr$_D^\bullet$ when generated upon the formation of $[P_{D1}P_{D2}]^+$.

Fig. 4 shows the spectra recorded 20 ns after the laser flash illumination in Mn-depleted Tyr_D-less PSII in PsbA1 (*i.e.* PsbA1/PsbD2-Y160F PSII) dark adapted for ~ 3-4 h at pH 8.6. The black spectrum was recorded after the first flash and the red spectrum is an average of the ΔI/I measured from the 5th to 10th laser flash illumination. The two spectra are very similar, if not identical, and, surprisingly, they are identical to the $[P_{D1}P_{D2}]^+$-*minus*-$[P_{D1}P_{D2}]$ difference spectra in the presence of $Tyr_D^\bullet$ and not to those in the presence of Tyr_D.

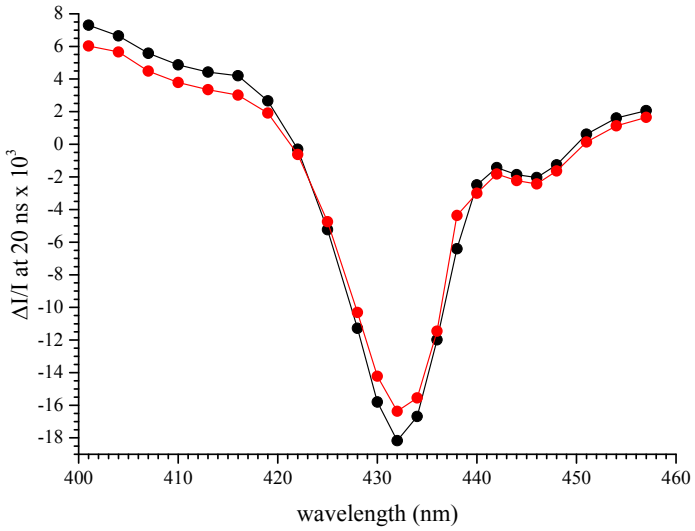

<u>Figure 4</u>: spectra recorded 20 ns after a laser flash illumination in Mn-depleted PsbA1/PsbD2-Y160F PSII dark adapted for 3-4 h at pH 8.6. The black full circles were recorded after the 1st flash and the red full circles are the average the measurements done from the 5th to the 10th 5 ns laser flash. The Chl concentration was 25 µg/ml and 100 µM PPBQ was added before the measurements.

It is clear from the results in Fig. 4 that the presence of $Tyr_D^\bullet$ is not required for the detection of the 440 nm to 460 nm double-trough spectral feature and is not directly responsible for this spectral feature. The structure around Tyr_D at pH 8.6 is unknown (see for example Hienerwadel et al. 2008) and the same is true when Tyr_D is replaced by phenylalanine in the Tyr_D-less mutant, however it seems possible that the local electrostatic environment in this mutant could mimic the situation occurring in presence of $Tyr_D^\bullet$. To test the effects of modifications in the H-bond network in this region, the spectra were recorded in two other mutants.

These two mutants were PsbA1-PsbD2/H189L single mutant (Un et al. 2007), in which the H-bonding histidine partner of Tyr_D is absent, and the PsbA1-PsbD2/Y160F-H189L double mutant (Sugiura et al. unpublished) in which both Tyr_D and its H-boning histidine partner are

absent. In the PsbA1-PsbD2/H189L single mutant, the oxidation of Tyr_D occurs with a very low efficiency, thus effectively $Tyr_D^{\bullet}$ cannot be formed. In this case, the spectra after the first flash and after the following flashes all correspond to a situation in which Tyr_D is present. In the PsbA1-PsbD2/Y160F-H189L double mutant, Tyr_D is absent and the H-bond network is expected to be modified compared to the PsbA1-PsbD2/Y160F single mutant. The results obtained in these two mutants are shown in Fig. 5. Panel A shows the spectra recorded in the PsbA1-PsbD2/H189L single mutant. Panel B shows the spectra recorded in the double mutant PsbA1-PsbD2/Y160F-H189L. The black full circles were recorded after the 1st flash and the red full circles are the average of the measurements done from the 5th to the 10th flash.

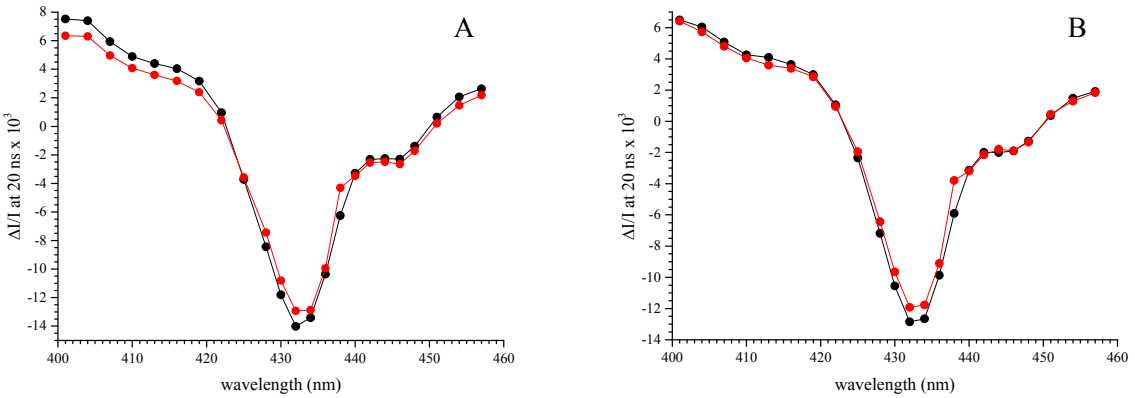

Figure 5: Spectra recorded 20 ns after a laser flash illumination in PsbA1-PsbD2/H189L PSII (Panel A) and in PsbA1-PsbD2/Y160F-H189L (Panel B). The samples were dark adapted for 3-4 h at pH 8.6 before the measurements. The black full circles were recorded after the 1st flash and the red full circles are the average the measurements done from the 5th to the 10th flash. The Chl concentration was 25 µg/ml and 100 µM PPBQ was added before the measurements.

In the PsbA1-PsbD2/H189L mutant, the spectral feature, which best seen as the trough at 446 nm, is present when Tyr_D is reduced (after both the 1st and subsequent flashes). This contrasts with the situation in PsbA1-PSII and PSbA3-PSII, where its formation required the presence of $Tyr_D^{\bullet}$. In the PsbA1-PsbD2/Y160F-H189L double mutant, the modification of the H-bond network due to loss of the Tyr_D and its H-bond partner, His 189, had no effect when compared with the PsbA1-PsbD2/Y160F single mutant. It should however be noted that when compared to the situation in PsbA1-PSII and PsbA3-PSII, the spectra between 432 nm and 440 nm appeared slightly broader on the longer wavelength side of the spectrum.

In the following, we address the situation in other mutants known to modify the spectral properties of P_{D1} and of some of the cofactors around it.

The first of these mutants is the PsbA3/H198Q, in which the His ligand of P_{D1} is replaced by a Gln, see Fig. 1. In this mutant, the $[P_{D1}P_{D2}]^{+}$-*minus*-$[P_{D1}P_{D2}]$ difference spectrum is shifted to the blue by ~ 3 nm (Diner et al. 2001, Sugiura et al. 2016). Despite this blue shift in the main bleach, the 440 nm to 460 nm spectral feature remained unaffected both in inactive (*i.e.* Mn-depleted) PSII from *Synechocystis* PCC6803 (Diner et al. 2001) at pH 5.9 and in O_2 evolving PSII from *T. elongatus* at pH 6.5 (Sugiura et al. 2016), with a trough at 446 nm in these two types of PSII.

The second mutant is the PsbA3/T179H in which the properties of Chl_{D1} are strongly modified (Schlodder et al. 2008, Takegawa et al. 2019). In this mutant, the Qy transition of Chl_{D1} is shifted to the red by ~ 2nm both in inactive PSII from *Synechocystis* PCC6803 (Schlodder et al. 2008) and in O_2 evolving PSII from *T. elongatus* at pH 6.5 (Takegawa et al. 2019). In the PsbA3/T179H *T. elongatus* mutant, the feature with a trough at 446 nm remained unaffected. However, this negative result can only be taken as inconclusive evidence against a role of Chl_{D1} in forming the spectral feature with the trough at 446 nm.

The third mutant on the D1 side is the PsbA3/E130Q mutant. The residue 130 of PsbA is H-bonded to the 13^1-keto of Phe_{D1}, affecting its midpoint potential and shifting its Qx band in the ~535-545 nm spectral region due to the changing strength of the H-bond (Merry et al. 1998, Sugiura et al. 2014). Fig. 6 shows that the 440 nm to 460 nm spectral feature *i*) remained unaffected in Mn-depleted PsbA3/E130Q PSII at pH 8.6 and *ii*) was absent on the first flash as in Mn-depleted PsbA3 PSII (Fig. 2). The data here show that the mysterious spectral feature in the Soret region does not seem to contain a contribution from a Phe_{D1} bandshift. However, it is not certain that a change in the Qx band of the absorption spectrum of Phe_{D1} would also be accompanied by a change in the Soret region (Sugiura et al. 2014).

Probing the modifications on the D2 side is more difficult. By comparing the electrochromic band-shifts of Phe_{D1} and Phe_{D2} in the Q_X band region around 550 nm, which are triggered by the formation of either $Tyr_Z^{\bullet}$ or $Tyr_D^{\bullet}$ in PsbA1-PSII and PsbA3-PSII, it was shown that the Q_X bandshift of Phe_{D2} induced by $Tyr_D^{\bullet}$ formation was slightly red shifted by 2-3 nm compared to the Phe_{D1} bandshift observed upon the formation of $Tyr_Z^{\bullet}$. This was interpreted by taking into account that the H-bonded residue to Phe_{D1} is a glutamate (PsbA1/E130) and the H-bonded residue to Phe_{D2} is a glutamine (PsbD/Q129) (Boussac et al. 2020). However, once again the conclusion remains tentative as a modification of the Qx band does not necessarily imply a change in the Soret region.

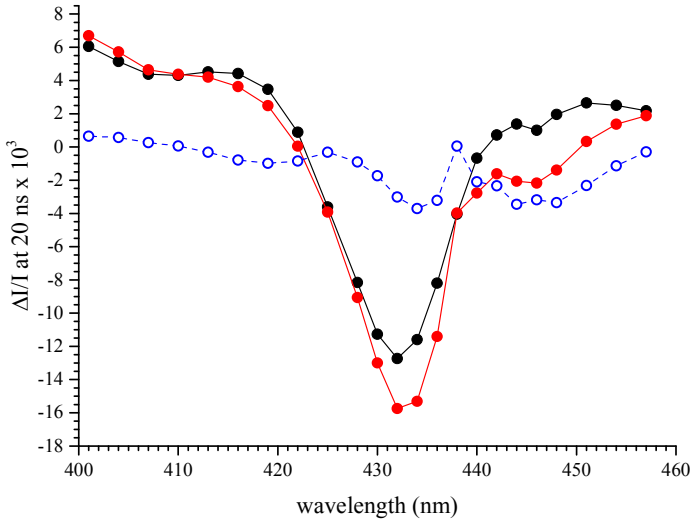

Figure 6: spectra recorded 20 ns after a laser flash illumination in Mn-depleted PsbA3/E130Q PSII, which was dark adapted for 3-4 h at pH 8.6. The black full circles were recorded after the 1st flash and the red full circles are the average the measurements done from the 5th to the 10th flash. The blue spectrum is the red spectrum minus the black spectrum. The Chl concentration was 25 µg/ml and 100 µM PPBQ was added before the measurements.

Fig. 7 shows the spectra recorded in a PsbA3-PsbD2/I178T mutant PSII (Sugiura et al. manuscript in preparation). The modifications of the Chl_{D2} in this mutant are expected to be comparable to those of the Chl_{D1} in the equivalent D1 mutation, *i.e.*, PsbA3/T179 (Takegawa et al. 2019). Fig. 7 shows again that there is no effect of the PsbD2/I178T mutation on the $(P_{D1}P_{D2})^{+}$-*minus*-$(P_{D1}P_{D2})$ spectra, and this is taken as an indication that Chl_{D2} is not the origin of the 440 nm to 460 nm double trough absorption feature.

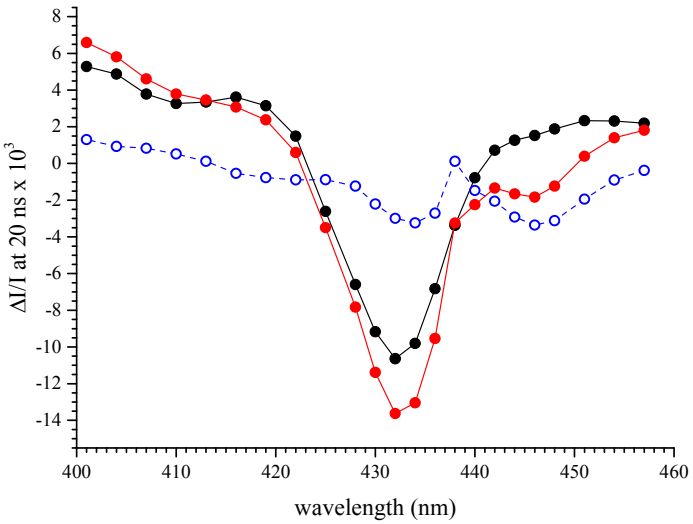

Figure 7: spectra recorded 20 ns after a laser flash illumination in Mn-depleted PsbA3-PsbD2/I178T PSII, which was dark adapted for 3-4 h at pH 8.6. The black full circles were recorded after the 1st flash and the red full circles are the average the measurements done from the 5th to the 10th flash. The blue spectrum is the red spectrum minus the black spectrum. The Chl concentration was 25 µg/ml and 100 µM PPBQ was added before the measurements.

Two other types of modified PSII from *T. elongatus* have been studied. Panel A of Fig. 8, shows that the 43H (His tagged) strain grown in the presence of 3-Fluorotyrosine. In the 43H PSII purified from these culture conditions, the tyrosine residues are all replaced by a 3-Fluorotyrosine (Rappaport et al. 2009). Despite that, there was no significant difference in the $[P_{D1}P_{D2}]^{+}$-*minus*-$[P_{D1}P_{D2}]$ spectra with respect to the spectra in Fig. 3, recorded with a normal PsbA1-PSII. The second PSII, in Panel B of Fig. 8, is a mutant in which the D1 protein is PsbA3 and in which the heme of Cyt*b*$_{559}$ is lacking (Sugiura et al. 2015). As the heme of Cyt*b*$_{559}$ has a Soret absorption in the spectral region studied here (Kaminskaya et al. 1999), a putative electrochromic band shift of either the reduced or the oxidized form of this heme was a possible candidate as the source of the 440-460 nm spectral feature. As it can be seen in Panel B of Fig. 8, this hypothesis can be definitely ruled out since the difference between the red and black spectra is similar to that in PsbA3-PSII.

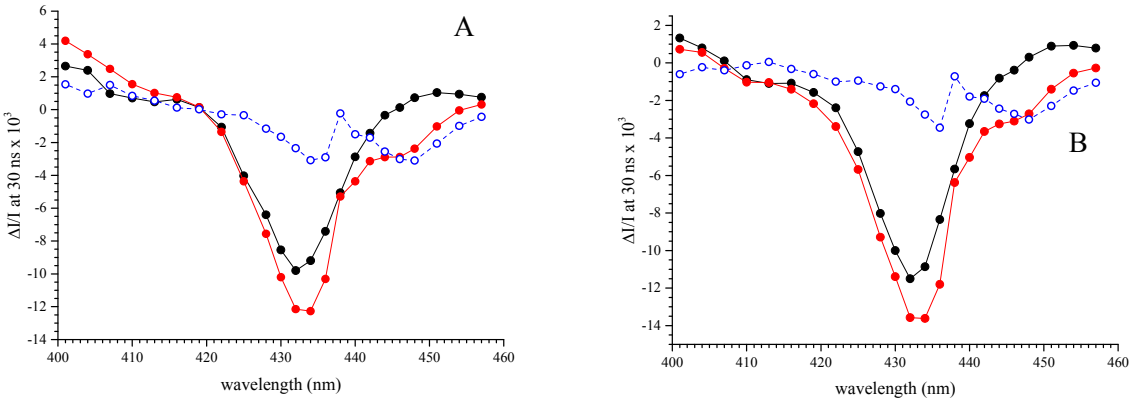

Figure 8: Spectra recorded 30 ns after a laser flash illumination in PsbA1-PSII containing 3-Fluorotyrosine (Panel A) and in the PsbA3/PsbE-H23A PSII (Panel B). The samples were dark adapted for 3-4 h at pH 8.6 before the measurements. The black full circles were recorded after the 1st flash and the red full circles are the average the measurements done from the 5th to the 10th flash. The blue spectra are the red spectra minus the black spectra. The Chl concentration was 25 µg/ml and 100 µM PPBQ was added before the measurements.

The same measurements were made in a PSII variant that has more significant modifications , namely PSII purified from *C. thermalis* grown under far-red light, in which Chl_{D1} is supposed to be either a Chl-*d* or a Chl-*f* (Nürnberg et al. 2018). A recent cryo-EM structure argued for Chl_{D1} being the Chl-*d* in the far-red PSII of *Synechococcus elongatus* PCC7335 (Gisriel et al. 2022). In addition to this Chl-*d/f* in the reaction centre, 4 Chl-*f* (or 1 Chl-*d* and 3 Chl-*f*) replace 4 of the others 34 Chl-*a*. The location of these additional antenna pigments in the far-red PSII of *C. thermalis* has not been determined experimentally yet, but candidates have been proposed based on structural considerations (Nürnberg et al 2018). For this sample, the spectra, shown in Fig. 9, were recorded 200 ns after the flashes. The first observation here is that the bleaching induced by the formation of $[P_{D1}P_{D2}]^+$ peaks at the same wavelength (~ 432 nm) as in Chl-*a* only PSII. It should be noted that in methanol, the Soret band of Chl-*f* is blue-shifted to ~ 400 nm and that of Chl-*d* is red-shifted to ~ 456 nm when compared to Chl-*a*, *e.g.* (Chen 2019). If, as seems likely, similar shifts in absorption occur also when these chlorophyll variants are located in the PSII reaction center, this would indicate that neither Chl-*f* or Chl-*d* would be involved in the $P_{D1}P_{D2}$ pair, in agreement with the suggestion of Nurnberg et al 2018, but discussed by Judd et al. 2020.

The decay of $[P_{D1}P_{D2}]^+$ in this Mn-depleted PSII at pH 8.6, and measured at 432 nm, occurred with a $t_{1/2}$ close to 200 ns as in PSII from *T. elongatus* (not shown). This implies that 200 ns after the first flash, approximately 25 % of the centers are in the $Tyr_D^\bullet$ state and 25 % in the $Tyr_Z^\bullet$ state. After the last flashes of the sequence, *i.e.* when $Tyr_D^\bullet$ is fully formed, at 200 ns after the flashes approximately 50 % of the centers are in the $Tyr_Z^\bullet$ state. This means that the spectral contributions of the electrochromic shifts triggered by the formation of $Tyr_D^\bullet$ and $Tyr_Z^\bullet$ are present in half of the centers on all the flashes and that their relative proportions differ after the first flash and the following flashes. This complication could be at the origin of the broader spectrum after the first flash in contrast to what is observed in all the other samples studied above. In addition, the shorter spacing between flashes used here (*i.e.* 300 ms *vs* 2 s) may affect the amplitude of the red spectrum. Nevertheless, the spectral differences between 440 and 460 nm remain clearly unaffected in this PSII with a trough at 446 nm observed predominantly after the 5^{th} to 10^{th} flash.

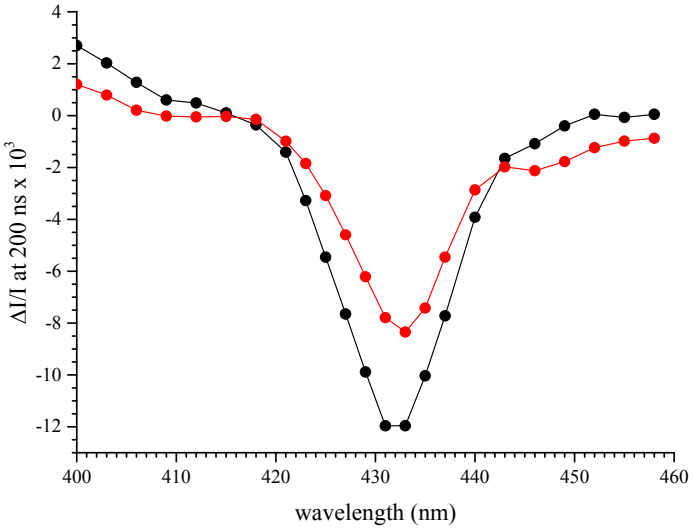

Figure 9: Spectra recorded 200 ns after each of a series of laser flash illuminations in Mn-depleted PSII purified from C. thermalis grown under far red light. The spacing between the 10 flashes of the sequence was 300 ms. The sample was dark adapted on ice for 2-3 h at pH 8.6 before the recording of the spectra. The black full circles were recorded after the 1st flash and the red full circles are the average the measurements done from the 5th to the 10th flash. The Chl concentration was 15 µg/ml and 100 µM PPBQ was added before the measurements

Conclusion

A range of PSII samples from mutants and variants (as listed in Table 1) all showed the double trough feature in the Soret region of the absorption spectrum when $[P_{D1}P_{D2}]^+$ was formed in the presence of $Tyr_D^\bullet$ (see Figure 2 blue spectrum). The double trough feature was seemingly unmodified in all of them, therefore there was no evidence for this spectral feature arising from P_{D1}, Chl_{D1}, Phe_{D1}, Phe_{D2}, Tyr_Z, Tyr_D and the Cyt*b*$_{559}$ heme. However, when Tyr_D was present in its native H-bonding environment and in its reduced form, the double trough feature was absent.

The most obvious candidate is P_{D2} as it is the pigment that is most closely associated with both P_{D1} and Tyr_D. It is also the only one that is untested spectroscopically. Mutants have been made and published but the relevant part of the Soret spectrum is unreported to our knowledge.

It was suggested earlier that when Tyr_D was reduced in the presence of $[P_{D1}P_{D2}]^+$, the redox equilibrium, $[P_{D1}^+ P_{D2}] \leftrightarrow [P_{D1}P_{D2}^+]$, is moved to the right (for electrostatic reasons), with the higher proportion of P_{D2}^+ favoring Tyr_D oxidation because of the shorter electron transfer distance. In contrast, this model seems to be contradicted by the data here: i) the mixed bleaching/band-shift features in the Soret region that is associated with $Tyr_D^\bullet$ may arise from

both P_{D1}^+ and P_{D2}^+ present in the sample at the same time due to the redox equilibrium; and ii) the more homogeneous spectrum associated with the presence of Tyr_D in its native H-bonding environment, is likely associated the pure (?) P_{D1}^+, presumably due to a change in the equilibrium. The mechanistic reason for this is unclear at present. This model can be tested by mutagenesis of P_{D2}.

Acknowledgements

This work has been in part supported by (i) the French Infrastructure for Integrated Structural Biology (FRISBI) ANR-10-INBS-05, (ii) the Labex Dynamo (ANR-11-LABX-0011-01), (iii) the JSPS-KAKENHI Grant in Scientific Research on Innovative Areas JP17H064351 and a JSPS-KAKENHI Grant 21H02447 and (iv) the BBSRC grants BB/R001383/1, BB/V002015/1 and BB/R00921X.

References

D. Béal, F. Rappaport, P. Joliot, A new high-sensitivity 10-ns time-resolution spectrophotometric technique adapted to in vivo analysis of the photosynthetic apparatus, Rev. Sci. Instrum. 70 (1999) 202–207. https://doi.org/10.1063/1.1149566

A. Boussac, A-L. Etienne, Spectral and kinetic pH-dependence of fast and slow Signal-II in Tris-washed chloroplasts, FEBS Lett. 148 (1982) 113–116. https://doi.org/10.1016/0014-5793(82)81254-4

A. Boussac, J. Sellés, M. Sugiura, What can we still learn from the electrochromic bandshifts in Photosystem II? Biochim. Biophys. Acta 1861 (2020) 148176. https://doi.org/10.1016/j.bbabio.2020.148176

A. Boussac, M. Sugiura, F. Rappaport, Probing the quinone binding site of Photosystem II from *Thermosynechococcus elongatus* containing either PsbA1 or PsbA3 as the D1 protein through the binding characteristics of herbicides, Biochim. Biophys. Acta 1807 (2010) 119–129. https://doi.org/10.1016/j.bbabio.2010.10.004

K. Brettel, E. Schlodder, H.T. Witt, Nanosecond reduction kinetics of photooxidized chlorophyll-a (P-680) in single flashes as a probe for the electron pathway, H^+ release and charge accumulation in the O_2-evolving complex, Biochim. Biophys. Acta 766 (1984) 403–415. https://doi.org/10.1016/0005-2728(84)90256-1

S. de Causmaecker, J.S. Douglass, A. Fantuzzi, W. Nitschke, A.W. Rutherford, Energetics of the exchangeable quinone, Q_B, in Photosystem II, Proc. Natl. Acad. Sci. USA 116 (2019) 19458–19463. https://doi.org/10.1073/pnas.1910675116

M. Chen, M. Schliep, R.D. Willows, Z-L. Cai, B.A. Neilan, H. Scheer, A Red-shifted chlorophyll, Science 329 (2010) 1318–1319. https://doi.org/10.1126/science.1191127

M. Chen, Chlorophylls d and f: Synthesis, occurrence, light-harvesting, and pigment organization in chlorophyll-binding protein complexes, Adv. Bot. Res. 90 (2019) 121–139. https://doi.org/10.1016/bs.abr.2019.03.006

H. Conjeaud, P. Mathis, The effect of pH on the reduction kinetics of P-680 in Tris-treatead chloroplasts, Biochim. Biophys. Acta 590 (1980) 353–359. https://doi.org/10.1016/0005-2728(80)90206-6

N. Cox, D.A. Pantazis, W. Lubitz, Current understanding of the mechanism of water oxidation in Photosystem II and its relation to XFEL data, Annual Review of Biochemistry 89 (2020) 795–820. https://doi.org/10.1146/annurev-biochem-011520104801

B.A. Diner, E. Schlodder, P.J. Nixon, W.J. Coleman, F. Rappaport, J. Lavergne, W.F.J. Vermaas, D.A. Chisholm, Site-directed mutations at D1-His198 and D2-His197 of Photosystem II in *Synechocystis* PCC 6803: sites of primary charge separation and cation and triplet stabilization, Biochemistry 24 (2001) 9265–9281. https://doi.org/10.1021/bi010121r

P. Faller, R.J. Debus, K. Brettel, M. Sugiura, A.W. Rutherford, A. Boussac, Rapid formation of the stable tyrosyl radical in photosystem II, Proc. Natl. Acad. Sci. USA 98 (2001) 14368–14373. https://doi.org/10.1073/pnas.251382598

C. Fufezan, C.-X. Zhang, A. Krieger-Liszkay, A.W. Rutherford, Secondary quinone in Photosystem II of *Thermosynechococcus elongatus*: Semiquinone-iron EPR signals and temperature dependence of electron transfer, Biochemistry 44 (2005) 12780–12789. https://doi.org/10.1021/bi051000k

F. Gan, S. Zhang, N.R. Rockwell, S.S. Martin, J.C. Lagarias, D.A. Bryant, Extensive remodeling of a cyanobacterial photosynthetic apparatus in far-red light, Science 345 (2014) 1312–1317. https://doi.org/10.1126/science.1256963

S. Gerken, K. Brettel, E. Schlodder, H.T. Witt, Direct observation of the immediate electron-donor to chlorophyll-a^{+} (P-680^{+}) in oxygen-evolving photosystem-complexes – Resolution of manosecond kinetics in the UV, FEBS Lett. 223 (1987) 376–380. https://doi.org/10.1016/0014-5793(87)80322-8

L.B. Giorgi, P.J. Nixon, S.A.P. Merry, D.M. Joseph, J.R. Durrant, J.D. Rivas, J. Barber, G. Porter, D.R. Klug, Comparison of primary charge separation in the photosystem II reaction center complex isolated from wild-type and D1-130 mutants of the cyanobacterium *Synechocystis* PCC 6803, J. Biol. Chem. 271 (1996) 2093–2101. https://doi.org/10.1074/jbc.271.4.2093

C.J. Gisriel, J. Wang, J. Liu, D.A. Flesher, K.M. Reiss, H-L. Huang, K.R. Yang, W.H. Armstrong, M.R. Gunner, V.S. Batista, R.J. Debus, G.W. Brudvig, High-resolution cryo-electron microscopy structure of Photosystem II from the mesophilic cyanobacterium, *Synechocystis* sp. PCC 6803, Proc. Natl. Acad. Sci. USA 119 (2022a) e2116765118. https://doi.org/10.1073/pnas.2116765118

C.J. Gisriel, G.Z. Shen, M-Y. Ho, V. Kurashov, D.A. Flesher, JM. Wang, A.W. Armstrong, J.H. Golbeck, M.R. Gunner, D.J. Vinyard, R.J. Debus, G.W. Brudvig, D.A. Bryant, Structure of a monomeric photosystem II core complex from a cyanobacterium acclimated to far-red light reveals the functions of chlorophylls d and f, J. Biol. Chem. 298 (2022b) 101424. https://doi.org/10.1016/j.jbc.2021.101424

R. Hienerwadel, B.A. Diner, C. Berthomieu, Molecular origin of the pH dependence of tyrosine D oxidation kinetics and radical stability in photosystem II, Biochim. Biophys. Acta 1777 (2008) 525–531. https://doi.org/10.1016/j.bbabio.2008.04.004

A.R. Holzwarth, M.G. Müller, M. Reus, M. Nowaczyk, J. Sander, M. Rögner, Kinetics and mechanism of electron transfer in intact Photosystem II and in the isolated reaction center: pheophytin is the primary electron acceptor, Proc. Natl. Acad. Sci. USA 103 (2006) 6895–6900. https://doi.org/10.1073/pnas.0505371103

P. Joliot, G. Barbieri, R, Chabaud, A new model of photochemical centers in system 2, Photochem. Photobiol. 10 (1969) 309–329. https://doi.Org/10.1111/j.1751-1097.1969.tb05696.x

M. Judd, J. Morton, D. Nürnberg, A. Fantuzzi, A.W. Rutherford, R. Purchase, N. Cox, E. Krausz, The primary donor of far-red photosystem II: Chl(D1) or P-D2? Biochim. Biophys. Acta 1861 (2020) 148248. https://doi.org/10.1016/j.bbabio.2020.148248

O. Kaminskaya, J. Kurreck, K.D. Irrgang, G. Renger, V.A. Shuvalov, Redox and spectral properties of cytochrome b(559) in different preparations of photosystem II, Biochemistry 49 (1999) 16223–16235. https://doi.org/10.1021/bi991257g

B. Kok, B. Forbush, M. McGloin, Cooperation of charges in photosynthetic O_2 evolution–I. A linear four step mechanism, Photochem. Photobiol. 11 (1970) 457–475. https://doi.org/10.1111/j.1751-1097.1970.tb06017.x

W. Lubitz, M. Chrysina, N. Cox, Water oxidation in Photosystem II, Photosynth. Res. 142 (2019) 105–125. https://doi.org/10.1007/s11120-019-00648-3

S.A.P. Merry, P.J. Nixon, L.M.C. Barter, M. Schilstra, G. Porter, J. Barber, J.R. Durrant, D.R. Klug, Modulation of quantum yield of primary radical pair formation in Photosystem II by site-directed mutagenesis affecting radical cations and anions, Biochemistry 37 (1998) 17439–17447. https://doi.org/10.1021/bi980502d

F. Müh, A. Zouni, Extinction coefficients and critical solubilisation concentrations of Photosystems I and II from *Thermosynechococcus elongatus*, Biochim. Biophys. Acta 1708 (2005) 219–228. https://doi.org/10.1016/j.bbabio.2005.03.005

D.J. Nurnberg, J. Morton, S. Santabarbara, A. Telfer, P. Joliot, L.A. Antonaru, A.V. Ruban, T. Cardona, E. Krausz, A. Boussac, A. Fantuzzi, A.W. Rutherford, Photochemistry beyond the red limit in chlorophyll f-containing photosystems, Science 360 (2018) 1210–1213. https://doi.org/10.1126/science.aar8313

S. Ogami, A. Boussac, M. Sugiura, Deactivation processes in PsbA1-Photosystem II and PsbA3-Photosystem II under photoinhibitory conditions in the cyanobacterium *Thermosynechococcus*

elongatus Biochim. Biophys. Acta 1817 (2012) 1322–1330. https://doi.org/10.1016/j.bbabio.2012.01.015

F. Rappaport, A. Boussac, D.A. Force, J. Peloquin, M. Brynda, M. Sugiura, S. Un, R.D Britt, B.A. Diner, Probing the coupling between proton and electron transfer in Photosystem II core complexes containing a 3-fluorotyrosine, J. Am. Chem. Soc. 131 (2009) 4425–4433. https://doi.org/10.1021/ja808604h

G. Renger, Mechanism of light induced water splitting in Photosystem II of oxygen evolving photosynthetic organisms, Biochim. Biophys. Acta 1817 (2012) 1164–1176. https://doi.org/10.1016/j.bbabio.2012.02.005

E. Romero, V.I. Novoderezhkin, R. van Grondelle, Quantum design of photosynthesis for bio-inspired solar-energy conversion, Nature 543 (2017) 355–365. https://doi.org/10.1038/nature22012

A.W. Rutherford, A. Boussac, P. Faller, The stable tyrosyl radical in Photosystem II: why D? Biochim. Biophys. Acta 1655 (2004) 222–230. https://doi.org/10.1016/j.bbabio.2003.10.016

E. Schlodder, T. Renger, G. Raszewski, W.J. Coleman, P.J. Nixon, R.O. Cohen, B.A. Diner, Site-directed mutations at D1-Thr179 of photosystem II in *Synechocystis* sp PCC 6803 modify the spectroscopic properties of the accessory chlorophyll in the D1-branch of the reaction center, Biochemistry 47 (2008) 3143–3154. https://doi.org/10.1021/bi702059f

A. Sedoud, N. Cox, M. Sugiura, W. Lubitz, A. Boussac, A.W. Rutherford, The semiquinone-iron complex of Photosystem II: EPR signals assigned to the low field edge of the ground state doublet of $Q_A^{\bullet}$-Fe^{2+} and $Q_B^{\bullet}$-Fe^{2+}, Biochemistry 50 (2011) 6012–6021. https://doi.org/10.1021/bi200313p

M. Suga, F. Akita, K. Hirata, G. Ueno, H. Murakami, Y. Nakajima, T. Shimizu, K. Yamashita, M. Yamamoto, H. Ago, J-R. Shen, Native structure of Photosystem II at 1.95 angstrom resolution viewed by femtosecond X-ray pulses, Nature (2015) 517: 99–103. https://doi.org/10.1038/nature13991

M. Sugiura, C. Azami, K. Koyama, A.W. Rutherford, F. Rappaport, A. Boussac, Modification of the pheophytin redox potential in *Thermosynechococcus elongatus* Photosystem II with PsbA3 as D1, Biochim. Biophys. Acta 1837 (2014) 139–148. https://doi.org/10.1016/j.bbabio.2013.09.009

M. Sugiura, A. Boussac, T. Noguchi, F. Rappaport, Influence of Histidine-198 of the D1 subunit on the properties of the primary electron donor, P680, of Photosystem II in *Thermosynechococcus elongatus*, Biochim. Biophys. Acta 1777 (2008) 331–342. https://doi.org/10.1016/j.bbabio.2008.01.007

M. Sugiura, Y. Inoue, Highly purified thermo-stable oxygen-evolving photosystem II core complex from the thermophilic cyanobacterium *Synechococcus elongatus* having his-tagged CP43, Plant Cell Physiol. 40 (1999) 1219–1231. https://doi.org/10.1093/oxfordjournals.pcp.a029510

M. Sugiura, M. Nakamura, K. Koyama, A. Boussac, Assembly of oxygen-evolving Photosystem II efficiently occurs with the apo-Cytb559 but the holo-Cytb559 accelerates the recovery of a functional enzyme upon photoinhibition, Biochim. Biophys. Acta 1847 (2015) 276–285. https://doi.org/10.1016/j.bbabio.2014.11.009

M. Sugiura, Y. Osaki, F. Rappaport, A. Boussac, Corrigendum to "Influence of Histidine-198 of the D1 subunit on the properties of the primary electron donor, P680, of Photosystem II in *Thermosynechococcus elongatus*" Biochim. Biophys. Acta 1857 (2016) 1943–1948. https://doi.org/10.1016/j.bbabio.2016.09.012

M. Sugiura, F. Rappaport, K. Brettel, T. Noguchi, A.W. Rutherford, A. Boussac, Site-directed mutagenesis of the *Thermosynechococcus elongatus* photosystem II: The O_2-evolving enzyme lacking the redox-active tyrosine D, Biochemistry 43 (2004) 13549–13563. https://doi.org/10.1021/bi048732h

Y. Takegawa, M. Nakamura, S. Nakamura, T. Noguchi, J. Sellés, A.W. Rutherford, A. Boussac, M. Sugiura, New insights on Chl_{D1} function in Photosystem II from site-directed mutants of D1/T179 in *Thermosynechococcus elongatus*, Biochim. Biophys. Acta 1860 (2019) 297–309. https://doi.org/10.1016/j.bbabio.2019.01.008

S. Un, A. Boussac, M. Sugiura, Characterization of the Tyrosine-Z radical and Its Environment in the Spin-Coupled $S_2Tyr_Z^{\bullet}$ State of Photosystem II from *Thermosynechococcus elongatus*, Biochemistry, 46 (2007) 3138–3150. https://doi.org/10.1021/bi062084f